Circular RNA MCTP2 Inhibits Cisplatin Resistance in Gastric Cancer by miR-99a-5p-Mediated Induction of MTMR3 Expression

Guangli Sun
Jiangsu Province Hospital and Nanjing Medical University First Affiliated Hospital
Zheng Li
Jiangsu Province Hospital and Nanjing Medical University First Affiliated Hospital
Zhongyuan He
Jiangsu Province Hospital and Nanjing Medical University First Affiliated Hospital
Weizhi Wang
Jiangsu Province Hospital and Nanjing Medical University First Affiliated Hospital
Sen Wang
Jiangsu Province Hospital and Nanjing Medical University First Affiliated Hospital
Xing Zhang
Jiangsu Province Hospital and Nanjing Medical University First Affiliated Hospital
Jiacheng Cao
Jiangsu Province Hospital and Nanjing Medical University First Affiliated Hospital
Penghui Xu
Jiangsu Province Hospital and Nanjing Medical University First Affiliated Hospital
Haixiao Wang
Jiangsu Province Hospital and Nanjing Medical University First Affiliated Hospital
Xiaoxu Huang
Jiangsu Province Hospital and Nanjing Medical University First Affiliated Hospital
Yiwen Xia
Jiangsu Province Hospital and Nanjing Medical University First Affiliated Hospital
Jialun Lv
Jiangsu Province Hospital and Nanjing Medical University First Affiliated Hospital
Zhe Xuan
Jiangsu Province Hospital and Nanjing Medical University First Affiliated Hospital
Tianlu Jiang
Jiangsu Province Hospital and Nanjing Medical University First Affiliated Hospital
Lang Fang
Jiangsu Province Hospital and Nanjing Medical University First Affiliated Hospital
Jing Yang

Jiangsu Province Hospital and Nanjing Medical University First Affiliated Hospital

Diancai Zhang

Jiangsu Province Hospital and Nanjing Medical University First Affiliated Hospital

Hao Xu

Jiangsu Province Hospital and Nanjing Medical University First Affiliated Hospital

Zekuan Xu (xuzekuan@njmu.edu.cn)

Jiangsu Province Hospital and Nanjing Medical University First Affiliated Hospital

---

Research

Keywords: GC, cisplatin, CircMCTP2, miR-99a-5p, MTMR3

Posted Date: August 2nd, 2020

DOI: https://doi.org/10.21203/rs.3.rs-49454/v1

Version of Record: A version of this preprint was published on November 17th, 2020. See the published version at https://doi.org/10.1186/s13046-020-01758-w.

Abstract

Background: Cisplatin (CDDP) is the first-line chemotherapy for gastric cancer (GC). Poor prognosis of GC patients is partially due to development of CDDP resistance. Circular RNAs (circRNAs) are a subclass of non-coding RNAs that function as microRNA (miRNA) sponges. The role of circRNAs in CDDP resistance in GC has not been evaluated.

Methods: RNA-sequencing was used to identify the differentially expressed circRNAs between the CDDP-resistant and CDDP-sensitive GC cells. qRT-PCR was used to detect the expression of circMCTP2 in GC tissues. The effects of circMCTP2 on CDDP resistance were investigated *in vitro* and *in vivo*. Pull-down assays and Luciferase reporter assays were performed to confirm the interaction among circMCTP2, miR-99a-5p, and myotubularin related protein 3 (MTMR3). The protein expression levels of MTMR3 were detected by western blotting. Autophagy was evaluated by confocal microscopy and transmission electron microscopy (TEM).

Results: CircMCTP2 was found to be downregulated in the CDDP-resistant GC cells and tissues as compared to that of the CDDP-sensitive ones. A high level of circMCTP2 was found to be a favorable factor for the prognosis of patients with GC. CircMCTP2 inhibited cell proliferation and autophagy while promoting apoptosis of CDDP-resistant GC cells in response to CDDP treatment. CircMCTP2 upregulated MTMR3 by sponging miR-99a-5p, and knockdown of MTMR3 could reverse the effects of circMCTP2 on CDDP resistance and autophagy of GC cells.

Conclusions: CircMCTP2 sensitizes GC to CDDP through the upregulation of MTMR3 by sponging miR-99a-5p. Overexpression of CircMCTP2 could be a new therapeutic strategy for counteracting CDDP resistance in GC.

Background

GC is one of the most common malignancies in the world, and is the fourth and fifth most prevalent malignancy in men and women, respectively [1]. In comparison with other areas in the world, GC is more common in East Asia with 43% of GC patients in China alone [2]. Despite improved treatment for GC, the prognosis of advanced GC patients remains poor with a low 5-year survival rate [3]. CDDP-based chemotherapy is the main treatment strategy for patients with advanced GC [4]. However, after several cycles of chemotherapy, 50% of the patients exhibit acquired drug resistance. The 5-year survival rate of these CDDP-resistant patients is only around 20% [5–7]. Thus, it is of great importance to elucidate the underlying molecular mechanisms involved in CDDP resistance in GC.

CircRNAs are a type endogenous non-coding RNAs that are characterized by closed loops [8]. It has been shown that circRNAs are produced from the back-splicing of pre-mRNA and they are conserved and stable because of their special structure [9, 10]. Recently, circRNAs have gathered growing attention as they have been found to act as miRNA sponges [11]. MiRNAs regulate gene expression by binding to the 3´-untranslated regions (3´-UTRs) [12]. Thus, through their action on miRNAs, circRNAs can regulate the

expression and biological functions of the target genes. CircRNAs play crucial roles in many types of carcinomas. CircNRIP1 promotes GC progression by sponging miR-149-5p [13]. CircMTO1 can inhibit the progression of hepatocellular carcinoma through the regulation of miR-9-mediated expression of p21 [14]. CircTP63 has been shown to contribute to the progression of lung squamous cell carcinoma by acting as sponge of miR-873-3p [15]. However, the relationship between circRNAs and CDDP-resistance in GC remains unknown.

It has been reported that miR-99a-5p is upregulated in CDDP-resistant GC cell lines as compared to that in their matched sensitive cell lines and promotes resistance of GC cells to CDDP [16]. MiR-99a-5p has also been verified to be negatively corelated with prognosis in patients with GC [17].

Autophagy is an intracellular system that removes damaged and unnecessary cellular components, such as damaged organelles and proteins, by delivering them to the lysosomes for degradation [18]. Accumulating studies have shown that autophagy is involved in CDDP resistance in different kinds of carcinomas [19, 20]. Inhibition of autophagy has also been reported to sensitize GC cells to CDDP [21, 22]. MTMR3 is one of the members of the myotubularin family. It is an inositol lipid 3phosphatase that can hydrolyze PtdIns3P (PI3P) [23]. PI3P is required for the process of autophagy [24]. The suppressive effect of MTMR3 on PI3P was found to inhibit the autophagosome formation [25]. Nevertheless, whether MTMR3 is involved in the regulation of CDDP resistance of GC cells has not been elucidated.

In this study, circMCTP2 was detected by RNA-sequencing as one of the circular RNAs that was downregulated in the CDDP-resistant GC cells as compared to the CDDP-sensitive ones. We report that circMCTP2 acts as miR-99a-5p sponge and sensitizes GC cells to CDDP through the upregulation of MTMR3. We believe that our findings may be helpful for the treatment for patients with CDDP-resistant GC.

Methods

Tissue samples

All GC tissues used in the research were obtained from the First Affiliated Hospital of Nanjing Medical University. All GC patients received CDDP-based chemotherapy after radical gastrectomy. We followed the method published earlier to divide patients into CDDP-resistant and CDDP-sensitive groups [26]. CDDP resistance implies GC recurrence during the CDDP-based treatment. Patients who showed no tumor recurrence during CDDP-based therapy were defined as CDDP-sensitive patients. The tissues used for RNA extraction and immunochemical staining were stored in liquid nitrogen and 4% formaldehyde, respectively.

Cell lines

BGC823, SGC7901, and SGC7901CDDP cell lines were purchased from the Cell Bank of Type Culture Collection of Chinese Academy of Sciences. BGC823CDDP cell line was established according to a

published protocol [27]. The four cell lines were cultured in RPMI1640 (Gibco, USA) at 37℃ with 5% carbon dioxide in an incubator.

RNA extraction and RNase R treatment

The Cytoplasmic and Nuclear RNA Purification Kit (Norgen Biotek, Canada) was used to extract nuclear and cytoplasmic RNAs. Total RNA from GC tissues and cells was extracted using the TRIzol reagent (Invitrogen, USA). The extracted total RNA of GC cell lines was mixed with 3 U/mg RNase R for 15 min at 37°C. qRT-PCR was performed to detect the expression of circMCTP2 and MCTP2 mRNA, which indicated the stability of circMCTP2 and MCTP2 mRNA.

Quantitative real-time polymerase chain reaction

mRNA was reverse transcribed into cDNA using the Prime script RT Reagent (Takara, Japan). For reverse transcription of miRNA, we used a New Poly(A) Tailing Kit (ThermoFisher Scientific, China). qRT-PCR was carried out with an ABI StepOne Plus system using the SYBR Green Master Mix (Roche, USA). The primers are listed in Additional file 1: Table S1.

Actinomycin D assay

GC cells (5×10^4 cells per well) were seeded into a 24-well plate. After 24 h, GC cells were mixed with 2 mg/L actinomycin D (Sigma-Aldrich, USA) for 0, 4, 8, 12, and 24 h. The stabilities of circRNA and mRNA were examined by qRT-PCR.

Fluorescence *in situ* hybridization (FISH)

We followed a previously published protocol to perform the assay [28]. We used a biotin-labeled probe for circMCTP2 and a Dig-labeled probe for miR-99a-5p (Exiqon, Denmark) in this assay. The signals of the biotin-labeled probe and the Dig-labeled probe were captured using Cy5-conjugated streptavidin and a tyramide-conjugated Alexa 488 fluorochrome TSA kit (ThermoFisher Scientific, China), respectively. Nuclei were stained with DAPI.

Cell transfection

Commercially available lentivirus-circMCTP2, lentivirus-miR-99a-5p mimics, lentivirus-miR-99a-5p inhibitor, and lentivirus-shMTMR3 were purchased from GenePharma (Shanghai, China). After transfection, we used puromycin (Solarbio, China) to establish stably transfected cell lines.

Cell counting kit-8 (CCK-8) cell viability assay

CCK-8 (Dojindo, Japan) was used to determine the cell viability of GC cells. GC cells were seeded into a 96-well plate at a density of 5000 cells per well. Seeded cells were incubated for 2 h with the CCK-8 reagent before measurement.

EDU assay

We performed the EDU assay to assess DNA synthesis, which indicated the cell proliferation of GC cells, using an EDU assay kit (RiboBio, China). Stained GC cells were photographed using a microscope (Nikon, Japan).

Flow cytometric analysis

GC cells were seeded at a density of 2×10^5 cells per well in a 6-well plate. After treating with CDDP for 48 h, a PI/ Annexin V Apoptosis Detection Kit (BD, USA) was used to stain the collected GC cells. The proportion of apoptotic GC cells was detected using a flow cytometer (Gallios, Beckman, USA).

Colony formation assay

GC cells were seeded into a 6-well plate at a density of 1000 cells per well. After being cultured for 14 days, crystal violet (Kaigen, China) was used to stain the fixed GC cells. The cells were washed with PBS and then the number of colonies were counted.

Luciferase reporter assay

Wild-type (wt) and mutant (mut) sequences of circMCTP2 were designed and inserted into the pGL-3 luciferase reporter vector (Realgene, China). BGC823CDDP and SGC7901CDDP were co-transfected with luciferase reporter plasmids and miR-99a-5p mimics. Firefly and renilla luciferase activities were determined using the Dual-Luciferase Reporter Assay System (Promega, USA).

RNA pull-down assay

The RNA pull-down assay was performed as per previously described methods [29]. RiboBio (Guangzhou, China) designed and synthesized the biotin-labeled probe specific to circMCTP2. GC cells were collected and sonicated to produce cell lysates. The lysate was incubated with circMCTP2 probe that was pre-bound on streptavidin-coupled Dynabeads (Invitrogen, USA) and oligo probe. The RNA mixture bound to the magnetic beads was rinsed with wash buffer and then extracted using the RNeasy Mini Kit (QIAGEN, Germany). We performed qRT-PCR on the RNA product. Biotinylated-miR-99a-5p and biotinylated-miR-NC were produced by GenePharma (Shanghai, China). After 48 h, the constructs were transfected into GC cells, and the cells were lysed. The lysate was incubated with streptavidin-coated magnetic beads and then rinsed with PBS. The biotin-coupled RNA complex was pulled down and subjected to qRT-PCR.

RNA immunoprecipitation assay

A Magna RNA immunoprecipitation (RIP) kit (Millipore, USA) was used to perform RIP assay. We used RIP buffer to lyse GC cells and the cell lysate was then incubated with magnetic beads conjugated with anti-Ago2 antibody (Millipore, USA) or IgG antibody. Finally, the immunoprecipitated RNA was extracted and subjected to qRT-PCR.

Transmission electron microscopy (TEM)

Prepared GC cells were harvested and a 2.5% solution of glutaraldehyde was used to fix GC cells overnight. Then, the GC cells were fixed with 1% OSO4 for 1 h. Samples were dehydrated with increasing concentrations of ethanol, followed by embedding in Epon. Sections were cut with a ultramicrotome and then stained with 0.3% lead citrate. A JEM-1010 electron microscope (JEOL, Japan) was used to observe autophagy in GC cells.

Confocal microscopy

GC cells transfected with GFP-mRFP-LC3 lentivirus (GeneChem, China) were seeded into a 35-mm culture dish for confocal microscopy. Hoechst was used to stain nucleus. Red and yellow puncta representing autolysosomes and autophagosomes, respectively, were detected by confocal microscopy (Carl Zeiss, Germany). Three random fields were selected for the quantification of puncta.

Western blotting

Total proteins were extracted from GC cells and tissues. The proteins were transferred to PVDF membrane (Millipore USA) after SDS-PAGE electrophoresis. After blocking in TBST buffer with 5% skimmed milk, the membranes were incubated with primary antibodies overnight at 4°C. The membranes were rinsed thrice with TBST and then incubated with secondary antibodies at room temperature for 2 h. After washing with TBST thrice, the bands were detected using an enhanced chemiluminescence detection system with Chemiluminescence HRP Substrate (Millipore, WBKL0100). Anti-Bcl2, anti-Bax, anti-caspase3, anti-c-caspase3, anti-β-actin, anti-P62, anti-Beclin1, anti-LC3, and anti-MTMR3 were purchased from Abcam (Cambridge, UK). Anti-rabbit IgG-HRP and anti-mouse IgG-HPR antibodies were obtained from Santa Cruz (Dallas, TX, USA).

Nude mice xenograft model

Female BALB/c nude mice (5 weeks old) were purchased from the Department of Laboratory Animal Center of Nanjing Medical University. Stably transfected GC cells (1×10^6) were injected subcutaneously into each armpit of a nude mouse. A week later, CDDP (5 mg/kg) was injected intraperitoneally into nude mice three times per week. All the nude mice were sacrificed at day 35.

TUNEL assay

We performed TUNEL assay to detect the rate of apoptosis in GC cells in nude mice subcutaneous tumors. The assay was carried out using a Cell Death Detection Kit (Roche, USA) and the TUNEL-positive cells were counted using a microscope (Nikon, Japan).

Immunochemical staining

Tissue samples from GC patients and subcutaneous tumors from nude mice were fixed with 4% formalin and embedded in paraffin. The sections were incubated with anti-ki67, anti-P62, and anti-MTMR3 overnight at 4°C. Then the sections were incubated with secondary antibody for 1 h at room temperature and developed with DAB solution for 3 min. The sections were counterstained with hematoxylin.

Statistical analysis

Statistical analysis was performed using SPSS software (version 19.0). $P < 0.05$ (*) or $P < 0.01$ (**) was considered statistically significant. We repeated all experiments thrice. The results are shown as mean ± standard deviation (SD). The Student's *t*-test and the Pearson's $\chi 2$ test were also used in the statistical analysis.

Results

CircMCTP2 is downregulated in CDDP-resistant GC cells and tissues

To identify the profile of differentially expressed circular RNA in CDDP-sensitive and CDDP-resistant GC cells, we performed RNA-seq analysis on BGC823 (CDDP-sensitive), BGC823CDDP (CDDP-resistant), SGC7901 (CDDP-sensitive), and SGC7901CDDP (CDDP-resistant) cells. Hundreds of circular RNAs were screened to be downregulated in CDDP-resistant GC cells, as compared to the expression levels in the CDDP-sensitive GC cells. We selected the top 50 downregulated circular RNAs each in BGC823CDDP and SGC7901CDDP and found 11 circular RNAs were downregulated in both BGC823CDDP and SGC7901CDDP (Fig. 1a). To further verify if these circular RNAs were reduced in the CDDP-resistant GC tissues, qRT-PCR was performed on 45 CDDP-sensitive and 15 CDDP-resistant GC tissues. Only six of them were decreased in the CDDP-resistant GC tissues and circMCTP2 (hsa_circ_0000657) was found to be the most downregulated circRNA (Fig. 1b). CircMCTP2 was determined to be reduced in CDDP-resistant GC cells by qRT-PCR too (Fig. 1c). We expanded the sample size of the GC tissues to 75 CDDP-sensitive and 25 CDDP-resistant GC tissues and then examined the expression levels of circMCTP2. CircMCTP2 was found to be downregulated in CDDP-resistant GC tissues with a larger sample size (Additional file 2: Figure S1a). The ROC curve was drawn according to the expression of circMCTP2 in the GC tissues (Additional file 2: Figure S1b). The area under curve (AUC) distinguishing CDDP-resistant and CDDP-sensitive patients was 0.9450, which implied that circMCTP2 could be a predictive biomarker for CDDP-resistance in GC. The patients with GC were divided into two groups based on the expression levels of circMCTP2 with 50 patients in each group. Based on the survival information we had collected earlier, DFS and OS curves were drawn. The patients with high expression of circMCTP2 showed a better prognosis compared to those in the low expression group (Additional file 2: Figure S1c and S1d). Clinicopathological characteristics showed that the expression of circMCTP2 was negatively corelated with tumor progression and CDDP resistance (Table 1).

Identification of circMCTP2 in GC

CircMCTP2 is derived from the MCTP2 locus that is located on chromosome 15. The head-to-tail structure of circMCTP2 was identified by Sanger sequencing (Fig. 1d). Convergent and divergent primers were designed for the amplification of linear MCTP2 and circMCTP2, respectively. As shown in Fig. 1e, circMCTP2 could be detected in cDNA under RNase R treatment, whereas linear MCTP2 was digested with RNase R. Linear MCTP2, rather than circMCTP2, could be detected in gDNA. Under RNase R treatment, circMCTP2 showed more stability than the MCTP2 mRNA (Fig. 1f). GC cells were treated with actinomycin D to further examine the stability of circMCTP2. As shown in Fig. 1g, circMCTP2 was more stable than the MCTP2 mRNA. The results of FISH assay revealed that circMCTP2 was predominantly located in the cytoplasm of GC cells (Fig. 1h). CircMCTP2 was also confirmed to be mainly localized within the cytoplasm by qRT-PCR (Fig. 1i). Based on these results, CircMCTP2 was found to be a stable cytoplasmic circRNA in GC cells.

CircMCTP2 inhibits CDDP-resistance of GC *in vitro*

As circMCTP2 was downregulated in CDDP-resistant GC cells, we transfected these two cell lines with lentivirus-circMCTP2. We observed that circMCTP2 was overexpressed in BGC823CDDP and SGC7901CDDP after lentivirus transfection whereas the level of MCTP2 mRNA was not affected (Additional file 3: Figure S2a and S2b). Overexpression of circMCTP2 reduced the viability of BGC823CDDP and SGC7901CDDP in response to treatment with different concentrations of CDDP (Fig. 2a and 2b). Elevated level of circMCTP2 decreased the number of colony formation in BGC823CDDP and SGC7901CDDP cells (Fig. 2c and 2d). As shown in Fig. 2e, CDDP-resistant GC cell proliferation was impaired by the overexpression of circMCTP2. Increased apoptosis induction in response to upregulation of circMCTP2 was detected in BGC823CDDP and SGC7901CDDP cells by flow cytometric analysis (Fig. 2f and 2g). The results of western blotting also showed that circMCTP2 could promote apoptosis of CDDP-resistant GC cells in response to CDDP treatment (Fig. 2h).

CircMCTP2 represses autophagy in CDDP-resistant GC cells

Enhancement of autophagy has been reported to contribute to CDDP resistance [30, 31]. We detected p62 by immunohistochemistry (IHC) and western blotting in CDDP-resistant and CDDP-sensitive GC tissues. As shown in Fig. 3a and 3b, p62 expression was lower in the CDDP-resistant patients, suggesting that autophagy might play a promotive role in CDDP resistance. Then, we investigated the effect of circMCTP2 on autophagy. We observed that the accumulation of GFP/mRFP-LC3 dots was repressed by the overexpression of circMCTP2 (Fig. 3c-3f). The expression of LC3-II protein was observed to be decreased by the overexpression of circMCTP2 (Fig. 3g). The results of transmission electron microscopy (TEM) also revealed that circMCTP2 could inhibit autophagy in CDDP-resistant GC cells (Fig. 3h and 3i).

CircMCTP2 acts as a sponge of miR-99a-5p

Three online databases, including miRanda, PITA, and RNAhybrid were used to predict the potential miRNAs that could be sponged by circMCTP2. The results of a microarray, which was conducted to detect miRNAs differentially expressed in the CDDP-sensitive and CDDP-resistant GC cells were

downloaded from GEO database (GSE86195). Eight miRNAs (miR-99a-5p, miR-324-5p, miR-485-5p, miR-149-5p, miR-708-5p, miR-452-5p, miR-188-5p, and miR-1285-3p) were predicted to be the potential targets of circMCTP2 and were upregulated in CDDP-resistant GC cells (Fig. 4a). We then performed the RNA pull-down assay using a biotin-labeled circMCTP2 probe. As shown in Fig. 4b, the pull-down efficiency was enhanced by the overexpression of circMCTP2. The expression levels of the candidate miRNA were examined by qRT-PCR after pull-down. MiR-99a-5p was pulled down by biotin-labeled circMCTP2 probe in the BGC823CDDP and SGC7901CDDP cells (Fig. 4c and 4d). The results of luciferase assay showed that the overexpression of miR-99a-5p could decrease the luciferase activity of wt circMCTP2 reporter rather than the mut circMCTP2 reporter, which indicated that miR-99a-5p could directly bind to circMCTP2. (Fig. 4e). The results of FISH assay revealed that circMCTP2 and miR-99a-5p were both localized to the cytoplasm of BGC823CDDP and SGC7901CDDP (Fig. 4f). We found miR-99a-5p was upregulated in the CDDP-resistant GC tissues by qRT-PCR (Fig. 4g). MiR-99a-5p was also found to be enhanced in the CDDP-resistant GC cells (Fig. 4h). Overexpression or knockdown of miR-99a-5p had no influence on the expression levels of circMCTP2 (Fig. 4i).

Knockdown of miR-99a-5p inhibits CDDP resistance of GC cells

Considering that miR-99a-5p is upregulated in BGC823CDDP and SGC7901CDDP, we transfected BGC823CDDP and SGC7901CDDP with lentivirus-miR-99a-5p inhibitor. The transfection efficiency was examined by qRT-PCR (Additional file 3: Figure S2c and S2d). The downregulation of miR-99a-5p repressed cell proliferation of BGC823CDDP and SGC7901CDDP (Additional file 4: Figure S3a and S3b). Then we performed flow cytometric analysis and western blotting to explore the influence of miR-99a-5p on cell apoptosis. We observed that apoptosis of CDDP-resistant GC cells was enhanced by the knockdown of miR-99a-5p (Additional file 4: Figure S3c and S3d).

MTMR3 is a direct target of miR-99a-5p

MTMR3 was predicted to be a potential target of miR-99a-5p in four online databases (miRDB, miRWalk, Targetscan and miRTarBase) (Fig. 5a). Additionally, previous studies have confirmed MTMR3 can inhibit autophagy [25]. Therefore, we hypothesized that MTMR3 might be a direct target of miR-99a-5p. Then we performed a luciferase reporter assay to confirm the binding of MTMR3 to miR-99a-5p in BGC823CDDP and SGC7901CDDP (Fig. 5b). The results of the pull-down assay also confirmed the interaction between miR-99a-5p and MTMR3 (Fig. 5c). Additionally, as shown in Fig. 5d, overexpressed miR-99a-5p caused an enrichment of MTMR3 in BGC823CDDP and SGC7901CDDP after Ago2 RIP. Knockdown of miR-99a-5p increased the expression levels of MTMR3 (Fig. 5e). Western blotting also confirmed that the protein expression levels of MTMR3 were negatively correlated to the expression of miR-99a-5p (Fig. 5f). MTMR3 was proved to be downregulated in CDDP-resistant GC cells (Fig. 5g and 5h). MTMR3 expression was also found to be reduced in CDDP-resistant GC tissues by qRT-PCR (Fig. 5i). It was observed in Fig. 5j that there was a negative correlation between the expression levels of miR-99a-5p and MTMR3. As shown in Fig. 5k-5n, MTMR3 expression was increased by circMCTP2 and this effect could be reversed by the

overexpression of miR-99a-5p. We confirmed that MTMR3 was directly targeted by miR-99a-5p and circMCTP2 could upregulate MTMR3 by sponging miR-99a-5p.

Knockdown of MTMR3 reverses the effect of circMCTP2 on CDDP-resistant GC cells

BGC823CDDP and SGC7901CDDP were transfected with lentivirus-shMTMR3 after the overexpression of circMCTP2. The expression levels of MTMR3 were examined by qRT-PCR and western blotting (Fig. 6a and 6b). As shown in Fig. 6c and 6d, decreased cell proliferation and colony forming ability of BGC823CDDP that was caused by the overexpression of circMCTP2 were restored by the knockdown of MTMR3. Similar results were obtained for SGC7901CDDP (Fig. 6e and 6f). The influence of circMCTP2 on the cell viability of BGC823CDDP and SGC7901CDDP was rescued by the downregulation of MTMR3 (Fig. 6g). The results of flow cytometric analysis and western blotting indicated that the effect of circMCTP2 on apoptosis of BGC823CDDP and SGC7901CDDP was rescued by the knockdown of MTMR3 (Fig. 6h-6j). To sum up, the downregulation of MTMR3 could counteract the effects of circMCTP2 on CDDP-resistant GC cells.

The effect of circMCTP2 on autophagy is reversed by the downregulation of MTMR3

To examine if the inhibitory effect of circMCTP2 on autophagy could be reversed by the knockdown of MTMR3, we performed confocal microscopy, TEM and, western blotting. The reduced accumulation of GFP/mRFP-LC3 dots caused by circMCTP2 was increased by the knockdown of MTMR3 in CDDP-resistant GC cells (Fig. 7a-7d). We could also observe that the decreased protein expression of LC3-II by circMCTP2 overexpression was restored by knockdown of MTMR3 (Fig. 7e and 7f). Similar results were observed by TEM analysis (Fig. 7g and 7h). Taken together, downregulation of MTMR3 could counteract the effect of circMCTP2 on autophagy in CDDP-resistant GC cells.

CircMCTP2 suppresses CDDP resistance of GC cells *in vivo*

To investigate the relationship between circMCTP2 and CDDP resistance *in vivo*, 1×10^6 CDDP-resistant GC cells transfected with NC or lentivirus-circMCTP2 were injected subcutaneously into each armpit of a nude mouse. CDDP (5 mg/kg) was injected intraperitoneally into nude mice three times per week. The proliferation rate of BGC823CDDP and SGC7901CDDP *in vivo* was reduced by the overexpression of circMCTP2 in response to CDDP treatment (Fig. 8a-8d). It was also found that the weight of the tumors was reduced by the overexpression of circMCTP2 (Fig. 8e). CircMCTP2 was detected to be overexpressed in the circMCTP2 groups compared to the NC groups (Fig. 8f). The results of IHC suggested that the percentage of ki67-positive cells was decreased by circMCTP2 (Fig. 8g). Meanwhile, the results of TUNEL assay revealed that circMCTP2 promoted apoptosis of CDDP-resistant GC cells *in vivo* (Fig. 8h). MTMR3 expression was observed to be positively corelated with the expression of circMCTP2 *in vivo* by IHC and western blotting (Fig. 8i, 8j). FISH assay was conducted on GC tissues and the results further confirmed circMCTP2 was lower in CDDP-resistant tissues compared to that in the CDDP-sensitive ones, whereas the expression of miR-99a-5p showed an opposite trend (Fig. 8k). MTMR3 was confirmed to be downregulated in CDDP-resistant GC tissues by IHC (Fig. 8l).

Discussion

Almost half of the GC cases and GC-related deaths worldwide occur in China [32]. CDDP is one of the most widely used drugs for chemotherapy [33]. Chemoresistance is a major cause of failure of chemotherapy to cure patients with cancer [34]. Understanding the mechanisms underlying resistance to CDDP in GC may contribute to a better treatment strategy for GC. Next generation sequencing (NGS) was performed on CDDP-resistant and CDDP-sensitive GC cells to identify the profile of circRNA. CircMCTP2 was selected as it showed a significant difference in its expression between the CDDP-resistant and CDDP-sensitive GC tissues. According to the follow-up data, patients with higher expression of circMCTP2 had better prognosis. The clinicopathological characteristics of the patients also revealed the correlation between circMCTP2 and CDDP resistance. We then carried out Rnase R and Actinomycin D assays to confirm the stable structure of circMCTP2. CircRNAs have rarely been reported to be associated with chemoresistance and we are the first to determine the role of circMCTP2 in CDDP resistance in GC.

To explore the effect of circMCTP2 on CDDP resistance in GC, we first performed colony formation and EDU assays. The results suggested that the overexpression of circMCTP2 could inhibit the proliferation of CDDP-resistant GC cells in response to CDDP treatment. Flow cytometric analysis and western blotting were then performed, and the results indicated that an upregulation of circMCTP2 could promote apoptosis of CDDP-resistant GC cells. CircRNAs exert functions in many pathologies by binding to RNA-binding proteins (RBPs) [35] and some can even encode proteins [36]. However, miRNA sponging is the most reported mechanism by which circRNAs function in tumors [37, 38]. To predict the potential downstream miRNA of circMCTP2, we combined the results of online databases and a microarray that was previously conducted to determine the miRNA profile of CDDP-resistant GC cells. By RNA pull-down assay, miR-99a-5p was then selected to be the possible miRNA which could be sponged by circMCTP2. Finally, we performed luciferase reporter assay to confirm the binding between miR-99a-5p and circMCTP2. The results of FISH assay revealed both circMCTP2 and miR-99a-5p localized to the cytoplasm of CDDP-resistant GC cells. MiR-99a-5p was validated to contribute to CDDP resistance by colony formation assay, EDU assay, flow cytometric analysis, and western blotting, which was consistent with the previously published study [16]. MTMR3 was calculated by online databases to be the downstream of miR-99a-5p, which was supported by the results of luciferase reporter, pull-down, and Ago2 RIP assays. CircMCTP2 was identified to upregulate MTMR3 by sponging miR-99a-5p, as observed by using qRT-PCR and western blotting. To further prove whether knockdown of MTMR3 could reverse the effect of circMCTP2, rescue experiments were carried out. The reduced proliferation and increased apoptosis of CDDP-resistant GC cells caused by circMCTP2 were counteracted by the knockdown of MTMR3.

Autophagy has been elucidated to promote tumor growth and chemoresistance [39].

MTMR3 was confirmed to reduce autophagic activity by acting as a PI3P phosphatase [25]. By IHC and western blotting, we found that P62, which is negatively related to autophagy, was downregulated in the CDDP-resistant GC tissues. We further detected autophagy in CDDP-resistant GC cells by confocal

microscopy, TEM, and western blotting. Results of these experiments showed that autophagy was inhibited by the overexpression of circMCTP2. The inhibitory effect of circMCTP2 on autophagy was also found to be reversed by the knockdown of MTMR3.

To examine the influence of circMCTP2 on CDDP resistance *in vivo*, xenograft tumor model was established with nude mice. CDDP was injected intraperitoneally three times a week according to the weight of nude mice. The volumes of the tumors with higher expression of circMCTP2 were found to be smaller than those of the control group. Based on the results of IHC and TUNEL assay, circMCTP2 could also suppress CDDP resistance *in vivo*.

There are limitations to this study. Expression of circMCTP2 was only detected in human GC tissues. Circulating circRNAs are reportedly better biomarkers for certain pathologies [40, 41]. In this study, plasma samples of the patients with GC were not collected, and thus we failed to analyze whether plasma circMCTP2 could be a suitable biomarker to distinguish CDDP-resistant GC patients from CDDP-sensitive patients. CircMCTP2 was only demonstrated to function as miRNA sponge, and whether circMCTP2 could regulate chemoresistance by binding to RBPs was not explored. MTMR3 was one of the targets of miR-99a-5p and we could not rule out the possibility that there might be other target genes. *Helicobacter pylori* has been acknowledged to be one of the most important pathogenic factors for GC [42]. It has also been reported that *H. pylori* can regulate CDDP resistance [43, 44]. Nevertheless, many of the patients did not receive *H. pylori* examination, so we did not analyze the relationship between *H. pylori* and circMCTP2.

Conclusion

CircMCTP2 has been demonstrated to be aberrantly downregulated in CDDP-resistant GC cells and tissues. Overexpression of circMCTP2 can sensitize GC cells to CDDP by sponging miR-99a-5p to restore the expression of MTMR3. Our findings may provide novel insights to counteract CDDP resistance during chemotherapy.

Abbreviations

qRT-PCR: quantitative real-time polymerase chain reaction; CDDP: cisplatin; circRNA: circular RNA; miRNA: microRNA; GC: gastric cancer; 3´-UTR: 3´-untranslated region; MTMR3: myotubularin related protein 3; PI3P: PtdIns3P; FISH: fluorescence *in situ* hybridization; TEM: transmission electron microscopy; DFS: disease-free survival; RIP: RNA immunoprecipitation; Bio-miR-99a-5p: biotinylated-miR-99a-5p; Bio-NC: biotinylated-miR-NC; OS: overall survival; gDNA: genomic DNA; IHC: immunohistochemistry; GEO: Gene Expression Omnibus; NGS: next generation sequencing; RBP: RNA-binding protein; SD: standard deviation.

Declarations

Ethics approval and consent to participate

The research was approved by the Ethics Committee of the First Affiliated Hospital of Nanjing Medical University. All patients recruited to the study signed written informed consents. The experiments concerning animals were approved by the Nanjing Medical University Ethics Committee.

Consent for publication

Not applicable.

Availability of data and materials

All data in our study will be available upon reasonable request.

Competing interests

The authors declare that they have no competing interests.

Funding

National Natural Science Foundation of China (81871946, 81902515); the Primary Research & Development Plan of Jiangsu Province (BE2016786); the Priority Academic Program Development of Jiangsu Higher Education Institutions (PAPD, JX10231801); Jiangsu Key Medical Discipline (General Surgery) (ZDXKA2016005); the Youth Fund of Jiangsu Natural Science Foundation (BK20181081).

Authors' contributions

ZX and GS designed the study. DZ and HX were responsible for quality control. GS, ZL, ZH, and WW performed the experiments. SW and XZ analyzed the data. GS wrote the manuscript.

Acknowledgements

Not applicable.

References

1. Torre LA, Bray F, Siegel RL, Ferlay J, Lortet-Tieulent J, Jemal A. Global cancer statistics, 2012. CA Cancer J Clin 2015; 65 (2): 87–108.
2. Yang L. Incidence and mortality of gastric cancer in China. World J Gastroenterol 2006; 12 (1): 17–20.
3. Catalano V, Labianca R, Beretta GD, Gatta G, de Braud F, Van Cutsem E. Gastric cancer. Crit Rev Oncol Hematol 2009; 71 (2): 127–64.
4. Van Cutsem E, Sagaert X, Topal B, Haustermans K, Prenen H. Gastric cancer. Lancet 2016; 388 (10060): 2654-2664.

5. Kamangar F, Dores GM, Anderson WF. Patterns of cancer incidence, mortality, and prevalence across five continents: defining priorities to reduce cancer disparities in different geographic regions of the world. J Clin Oncol 2006; 24 (14): 2137-50.
6. Longley DB, Harkin DP, Johnston PG. 5-fluorouracil: mechanisms of action and clinical strategies. Nat Rev Cancer 2003; 3 (5): 330–8.
7. Shah MA. Update on metastatic gastric and esophageal cancers. J Clin Oncol 2015; 33 (16): 1760–9.
8. Wilusz JE, Sharp PA. Molecular biology. A circuitous route to noncoding RNA. Science 2013; 340 (6131): 440-1.
9. Memczak S, Jens M, Elefsinioti A, Torti F, Krueger J, Rybak A, et al. Circular RNAs are a large class of animal RNAs with regulatory potency. Nature 2013; 495 (7441): 333–8.
10. Szabo L, Morey R, Palpant NJ, Wang PL, Afari N, Jiang C, et al. Statistically based splicing detection reveals neural enrichment and tissue-specific induction of circular RNA during human fetal development. Genome Biol 2015; 16: 126.
11. Kulcheski FR, Christoff AP, Margis R. Circular RNAs are miRNA sponges and can be used as a new class of biomarker. J Biotechnol 2016; 238: 42–51.
12. Sun G, Li Z, Wang W, Chen Z, Zhang L, Li Q, et al. miR-324-3p promotes gastric cancer development by activating Smad4-mediated Wnt/beta-catenin signaling pathway. J Gastroenterol 2018; 53 (6): 725-739.
13. Zhang X, Wang S, Wang H, Cao J, Huang X, Chen Z, et al. Circular RNA circNRIP1 acts as a microRNA-149-5p sponge to promote gastric cancer progression via the AKT1/mTOR pathway. Mol Cancer 2019; 18 (1): 20.
14. Han D, Li J, Wang H, Su X, Hou J, Gu Y, et al. Circular RNA circMTO1 acts as the sponge of microRNA-9 to suppress hepatocellular carcinoma progression. Hepatology 2017; 66 (4): 1151-1164.
15. Cheng Z, Yu C, Cui S, Wang H, Jin H, Wang C, et al. circTP63 functions as a ceRNA to promote lung squamous cell carcinoma progression by upregulating FOXM1. Nat Commun 2019; 10 (1): 3200.
16. Zhang Y, Xu W, Ni P, Li A, Zhou J, Xu S. MiR-99a and MiR-491 Regulate Cisplatin Resistance in Human Gastric Cancer Cells by Targeting CAPNS1. Int J Biol Sci 2016; 12 (12): 1437-1447.
17. Zhang C, Zhang CD, Ma MH, Dai DQ. Three-microRNA signature identified by bioinformatics analysis predicts prognosis of gastric cancer patients. World J Gastroenterol 2018; 24 (11): 1206-1215.
18. Mizushima N, Komatsu M. Autophagy: renovation of cells and tissues. Cell 2011; 147 (4): 728–41.
19. He J, Yu JJ, Xu Q, Wang L, Zheng ZJ, Liu LZ, et al. Downregulation of ATG14 by EGR1-MIR152 sensitizes ovarian cancer cells to cisplatin-induced apoptosis by inhibiting cyto-protective autophagy. Autophagy 2015; 11 (2): 373-84.
20. Song J, Qu Z, Guo X, Zhao Q, Zhao X, Gao L, et al. Hypoxia-induced autophagy contributes to the chemoresistance of hepatocellular carcinoma cells. Autophagy 2009; 5 (8): 1131-44.

21. Zhao J, Nie Y, Wang H, Lin Y. MiR-181a suppresses autophagy and sensitizes gastric cancer cells to cisplatin. Gene 2016; 576 (2 Pt 2): 828-33.
22. Dong X, Wang Y, Zhou Y, Wen J, Wang S, Shen L. Aquaporin 3 facilitates chemoresistance in gastric cancer cells to cisplatin via autophagy. Cell Death Discov 2016; 2: 16087.
23. Walker DM, Urbé S, Dove SK, Tenza D, Raposo G, Clague MJ. Characterization of MTMR3. an inositol lipid 3-phosphatase with novel substrate specificity. Curr Biol 2001; 11 (20): 1600-5.
24. Simonsen A, Tooze SA. Coordination of membrane events during autophagy by multiple class III PI3-kinase complexes. J Cell Biol 2009; 186 (6): 773-82.
25. Taguchi-Atarashi N, Hamasaki M, Matsunaga K, Omori H, Ktistakis NT, Yoshimori T, et al. Modulation of local PtdIns3P levels by the PI phosphatase MTMR3 regulates constitutive autophagy. Traffic 2010; 11 (4): 468-78.
26. Bagrodia A, Lee BH, Lee W, Cha EK, Sfakianos JP, Iyer G, et al. Genetic determinants of cisplatin resistance in patients with advanced germ cell tumors. J Clin Oncol 2016; 34 (33): 4000–7.
27. Li B, Wang W, Li Z, Chen Z, Zhi X, Xu J, et al. MicroRNA-148a-3p enhances cisplatin cytotoxicity in gastric cancer through mitochondrial fission induction and cyto-protective autophagy suppression. Cancer Lett 2017; 410: 212–27.
28. Zheng Q, Bao C, Guo W, Li S, Chen J, Chen B, et al. Circular RNA profiling reveals an abundant circHIPK3 that regulates cell growth by sponging multiple miRNAs. Nat Commun 2016; 7: 11215.
29. Li Y, Zheng F, Xiao X, Xie F, Tao D, Huang C, et al. CircHIPK3 sponges miR-558 to suppress heparanase expression in bladder cancer cells. EMBO Rep 2017; 18 (9): 1646–59.
30. Zhou F, Yang X, Zhao H, Liu Y, Feng Y, An R, et al. Down-regulation of OGT promotes cisplatin resistance by inducing autophagy in ovarian cancer. Theranostics 2018; 8 (19): 5200-5212.
31. Pan X, Chen Y, Shen Y, Tantai J. Knockdown of TRIM65 inhibits autophagy and cisplatin resistance in A549/DDP cells by regulating miR-138-5p/ATG7. Cell Death Dis 2019; 10 (6): 429.
32. Nie Y, Wu K, Yu J, Liang Q, Cai X, Shang Y, et al. A global burden of gastric cancer: the major impact of China. Expert Rev Gastroenterol Hepatol 2017; 11 (7): 651–61.
33. Florea A-M, Büsselberg D. Cisplatin as an anti-tumor drug: cellular mechanisms of activity, drug resistance and induced side effects. Cancers 2011; 3 (1): 1351–71.
34. Brabec V, Kasparkova J. Modifications of DNA by platinum complexes. Relation to resistance of tumors to platinum antitumor drugs. Drug Resist Updat 2005; 8 (3): 131–146.
35. Qu S, Zhong Y, Shang R, Zhang X, Song W, Kjems J, et al. The emerging landscape of circular RNA in life processes. RNA Biol 2017; 14 (8): 992-999.
36. Dong Y, He D, Peng Z, Peng W, Shi W, Wang J, et al. Circular RNAs in cancer: an emerging key player. J Hematol Oncol 2017; 10 (1): 2.
37. Liu W, Ma W, Yuan Y, Zhang Y, Sun S. Circular RNA hsa_circRNA_103809 promotes lung cancer progression via facilitating ZNF121-dependent MYC expression by sequestering miR-4302. Biochem Biophys Res Commun 2018; 500 (4): 846–851.

38. He JH, Li YG, Han ZP, Zhou JB, Chen WM, Lv YB, et al. The CircRNA-ACAP2/Hsa-miR-21-5p/ Tiam1 regulatory feedback circuit affects the proliferation, migration, and invasion of colon cancer SW480 cells. Cell Physiol Biochem 2018; 49 (4): 1539–1550.
39. Shteingauz A, Boyango I, Naroditsky I, Hammond E, Gruber M, Doweck I, et al. Heparanase Enhances Tumor Growth and Chemoresistance by Promoting Autophagy. Cancer Res 2015; 75 (18): 3946-57.
40. Hang D, Zhou J, Qin N, Zhou W, Ma H, Jin G, et al. A novel plasma circular RNA circFARSA is a potential biomarker for nonsmall cell lung cancer. Cancer Med 2018; 7 (6): 2783–91.
41. Zhang J, Xu Y, Xu S, Liu Y, Yu L, Li Z, et al. Plasma circular RNAs, Hsa_circRNA_025016, predict postoperative atrial fibrillation after isolated off-pump coronary artery bypass grafting. J Am Heart Assoc 2018; 7: e006642.
42. Amieva M, Peek RM Jr. Pathobiology of Helicobacter pylori induced gastric cancer. Gastroenterology 2016; 150 (1): 64–78.
43. Shao L, Chen Z, Soutto M, Zhu S, Lu H, Romero-Gallo J, et al. Helicobacter pylori-induced miR-135b-5p promotes cisplatin resistance in gastric cancer. Faseb j 2019; 33 (1): 264-274.
44. Zhou X, Su J, Zhu L, Zhang G. Helicobacter pylori modulates cisplatin sensitivity in gastric cancer by down-regulating miR-141 expression. Helicobacter 2014; 19 (3): 174-81.

Table

Table1: Expression of circMCTP2 in human gastric cancer and the clinicopathological characteristics of the patients'

Characteristics	Number	circMCTP2 expression		P-value
		High group	Low group	
Age(years)				
≥60	61	32	29	0.539
<60	39	18	21	
Gender				
Male	68	32	36	0.391
Female	32	18	14	
Size(cm)				
≥3(cm)	57	21	36	0.002**
<3(cm)	43	29	14	
Stage				
II	42	26	16	0.043*
III	58	24	34	
T grade				
T_1+T_2	36	23	13	0.037*
T_3+T_4	64	27	37	
Lymph node metastasis				
N1-N3	87	41	46	0.137
N0	13	9	4	
CDDP chemosensitivity				
Sensitive	75	48	27	<0.001**
Resistant	25	2	23	

*p<0.05 and **p<0.01 Statistically significant difference

Figures

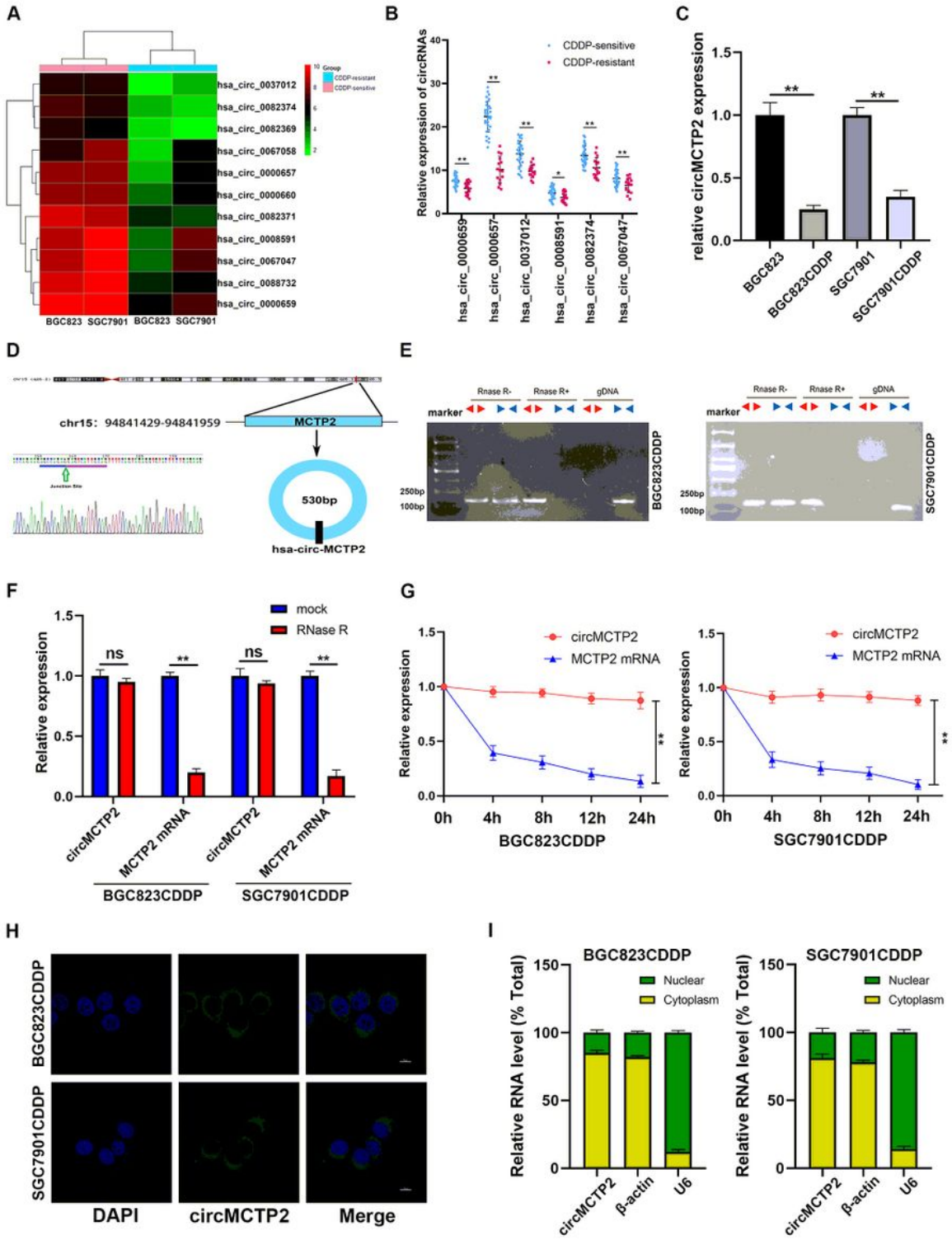

Figure 1

CircMCTP2 expression is down-regulated in CDDP-resistant GC tissues and cells. a Heatmap of circular RNAs downregulated in BGC823CDDP and SGC7901CDDP compared to those in CDDP-sensitive GC cells. b Identification of circular RNAs decreased in CDDP-resistant GC tissues by qRT-PCR. c Expression of circMCTP2 in CDDP-resistant and CDDP-sensitive GC cells by qRT-PCR. d Head-to-tail splicing of circMCTP2 was confirmed with Sanger-sequencing. e Back-spliced and linear MCTP2 were detected in

cDNA with or without RNase R and genomic DNA (gDNA) by RT-PCR. f CircMCTP2 and MCTP2 mRNA were treated with RNase R to detect their stability. g Results of actinomycin D assay. h CircMCTP2 was validated by FISH assay to be preferentially located in cytoplasm of GC cells. i CircMCTP2 was confirmed to be mainly localized within the cytoplasm of GC cells by qRT-PCR. (*p<0.05, **p<0.01. Data are expressed as mean ± SD).

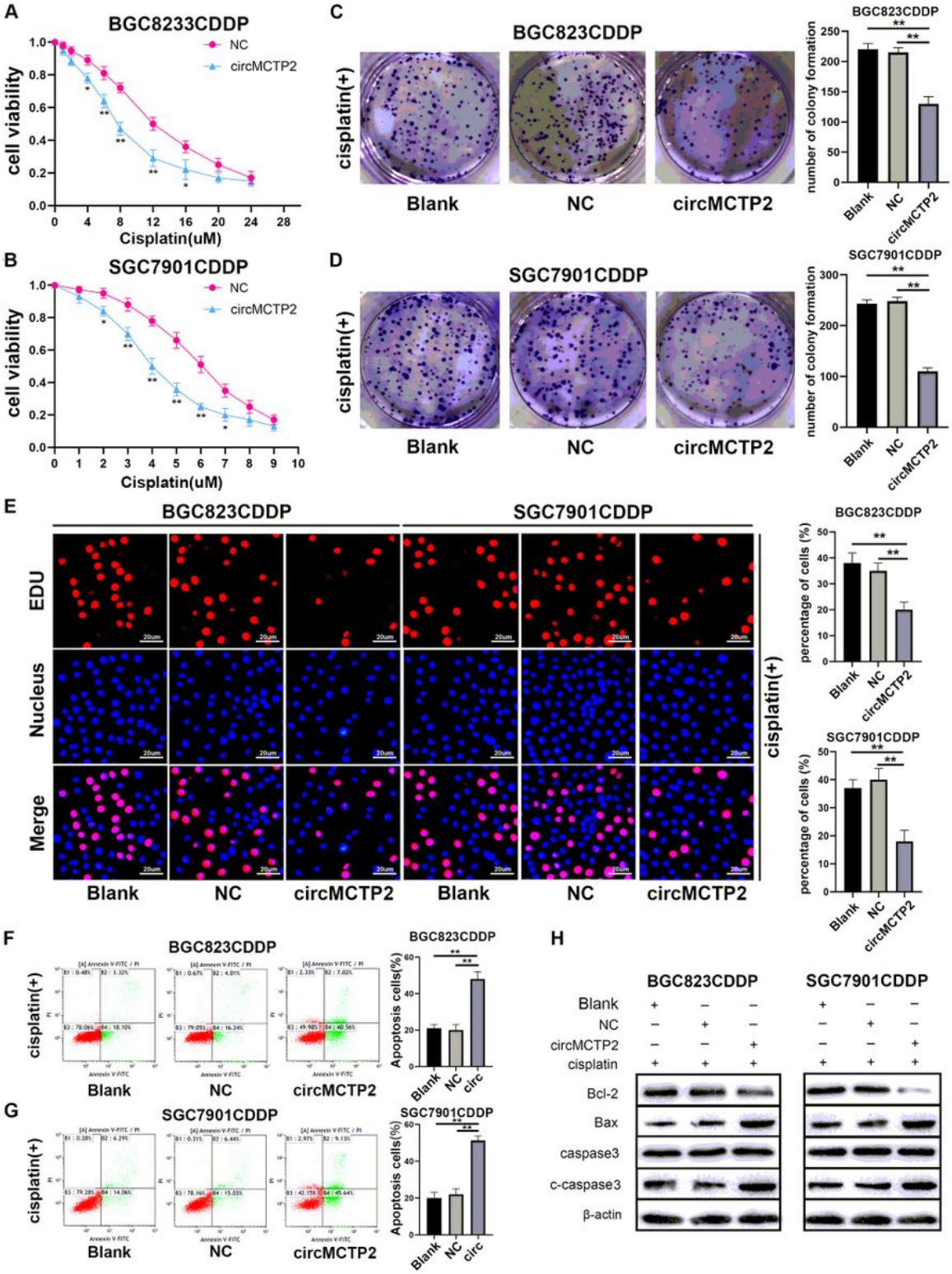

Figure 2

Overexpression of circMCTP2 facilitates sensitivity of CDDP-resistant GC cells in vitro. a and b Cell viability of CDDP-resistant GC cells was reduced by elevated expression of circMCTP2. c Overexpression of circMCTP2 impaired the colony-forming ability of BGC823CDDP in response to cisplatin treatment. d CircMCTP2 decreased colony formation of SGC7901CDDP in the presence of cisplatin. e Assessment of DNA synthesis of BGC823CDDP and SGC7901CDDP transfected with NC and lentivirus-circMCTP2 in presence of cisplatin. f and g Apoptosis of CDDP-resistant GC cells treated with cisplatin was determined by flow cytometric analysis. h Apoptosis-related proteins were detected by western blotting on BGC823CDDP and SGC7901CDDP. CDDP treatment: 12 μM, 48 h for BGC823CDDP and 6 μM, 48 h for SGC7901CDDP. (*$p<0.05$, **$p<0.01$. Data are expressed as mean ± SD).

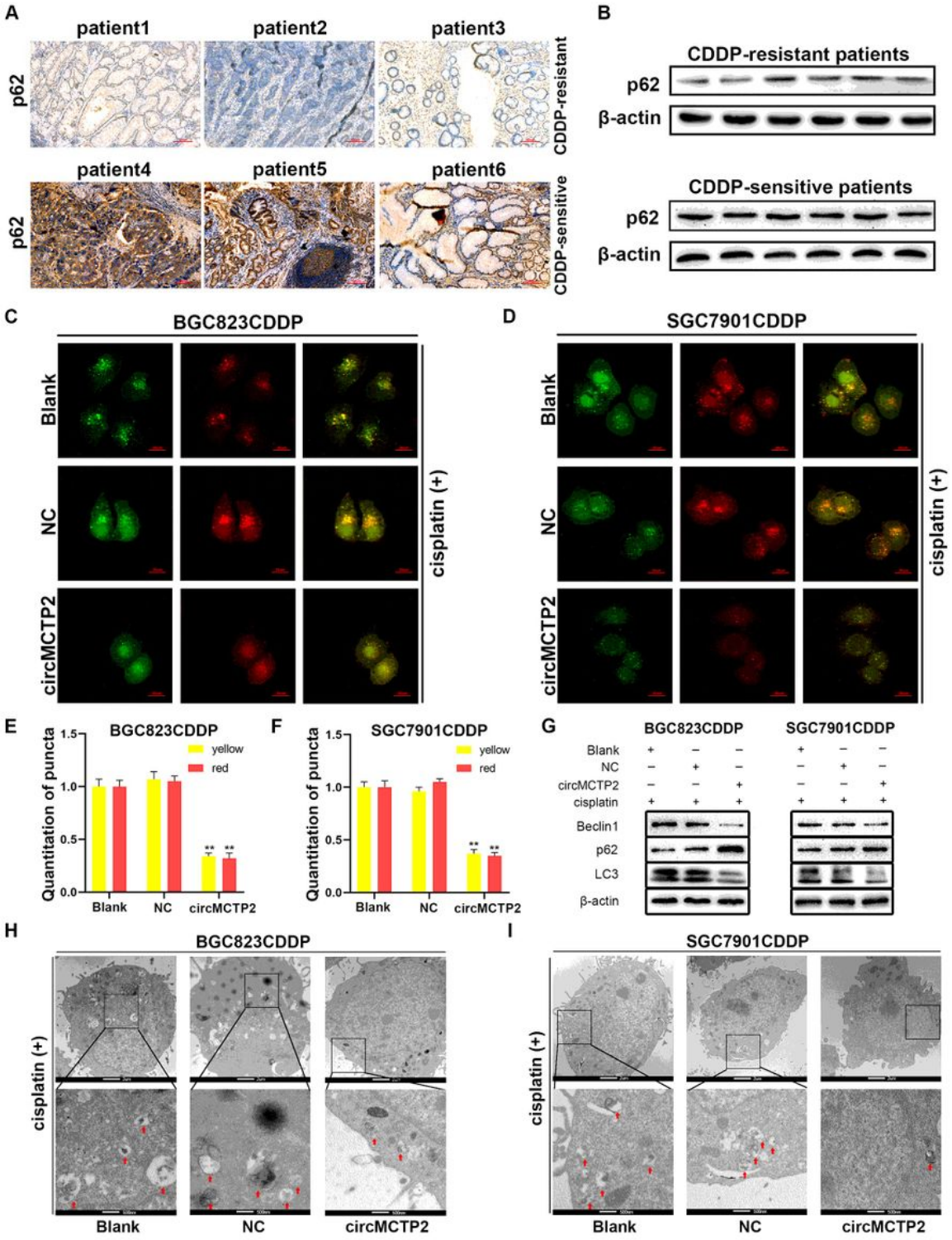

Figure 3

CircMCTP2 represses autophagy in CDDP-resistant GC cells. a Expression of p62 protein was lower in CDDP-resistant GC patients compared to that in the CDDP-sensitive ones. b Expression levels of p62 were detected in GC tissues by western blotting. c-f GFP/ mRFP-LC3 dots were observed and counted by confocal microscopy. g Protein levels of Beclin1, p62, and LC3-II were examined by western blotting. h and i Autophagic microstructure of CDDP-resistant GC cells was observed by transmission electron

microscopy. CDDP treatment: 12 μM, 48 h for BGC823CDDP and 6 μM, 48 h for SGC7901CDDP. (*p<0.05, **p<0.01. Data expressed as mean ± SD).

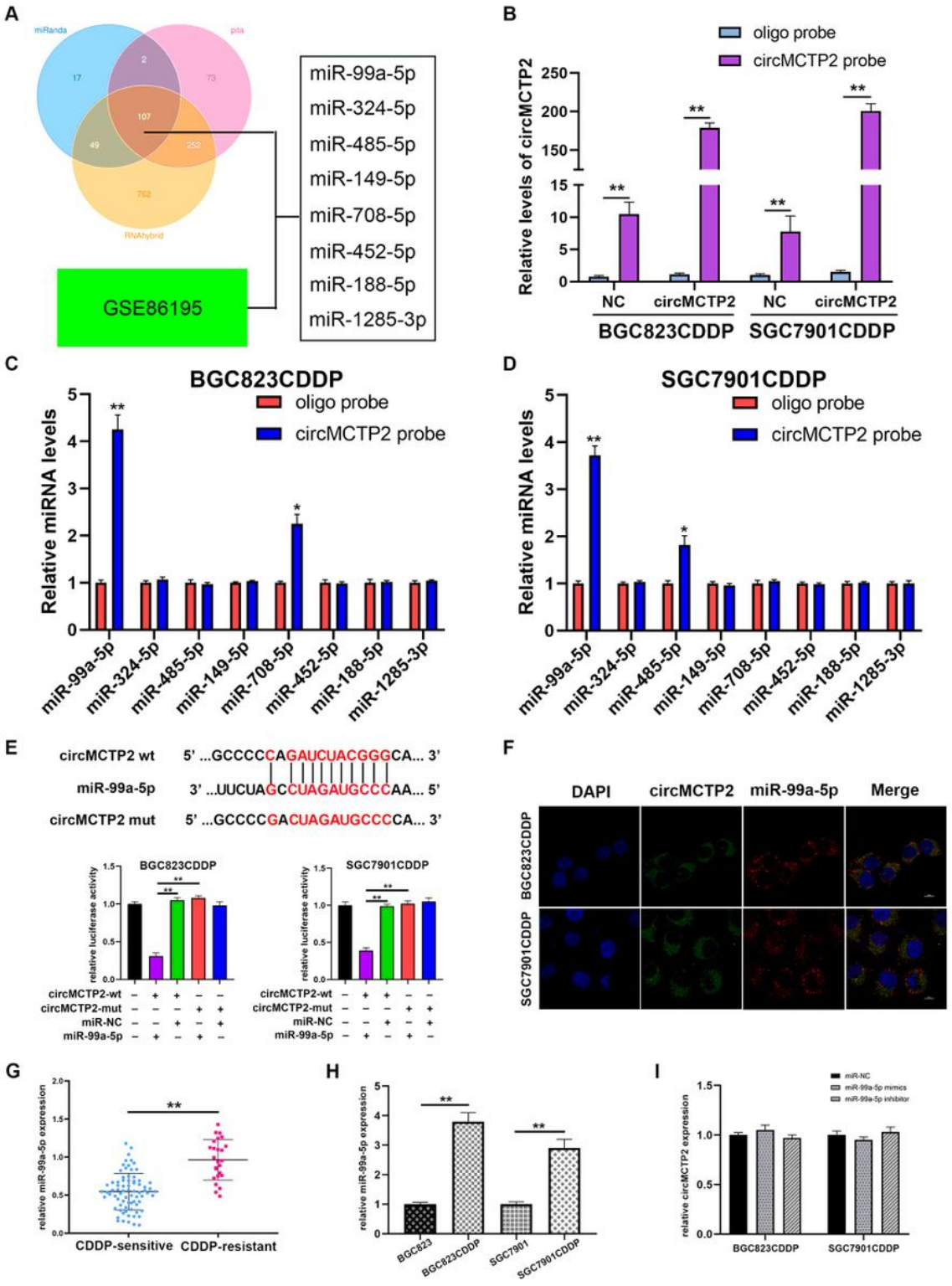

Figure 4

CircMCTP2 serves as a miRNA sponge of miR-99a-5p. a Candidate miRNAs predicted to be the potential binding targets of circMCTP2. b qRT-PCR analysis to examine the expression of circMCTP2 in lysates of BGC823CDDP and SGC7901CDDP. c and d qRT-PCR analysis to examine the expression of candidate

miRNAs after pull-down assay e Luciferase activity analyzed in BGC823CDDP and SGC7901CDDP transfected with miR-NC or miR-99a-5p mimics and wt or mut circMCTP2. f CircMCTP2 and miR-99a-5p were localized to the cytoplasm of CDDP-resistant GC cells by FISH assay. g MiR-99a-5p was detected to be upregulated in CDDP-resistant GC tissues by qRT-PCR. h MiR-99a-5p was detected to be upregulated in CDDP-resistant GC cells by qRT-PCR. i Overexpression or knockdown of miR-99a-5p did not affect the expression of circMCTP2. (*p<0.05, **p<0.01. Data are expressed as mean ± SD).

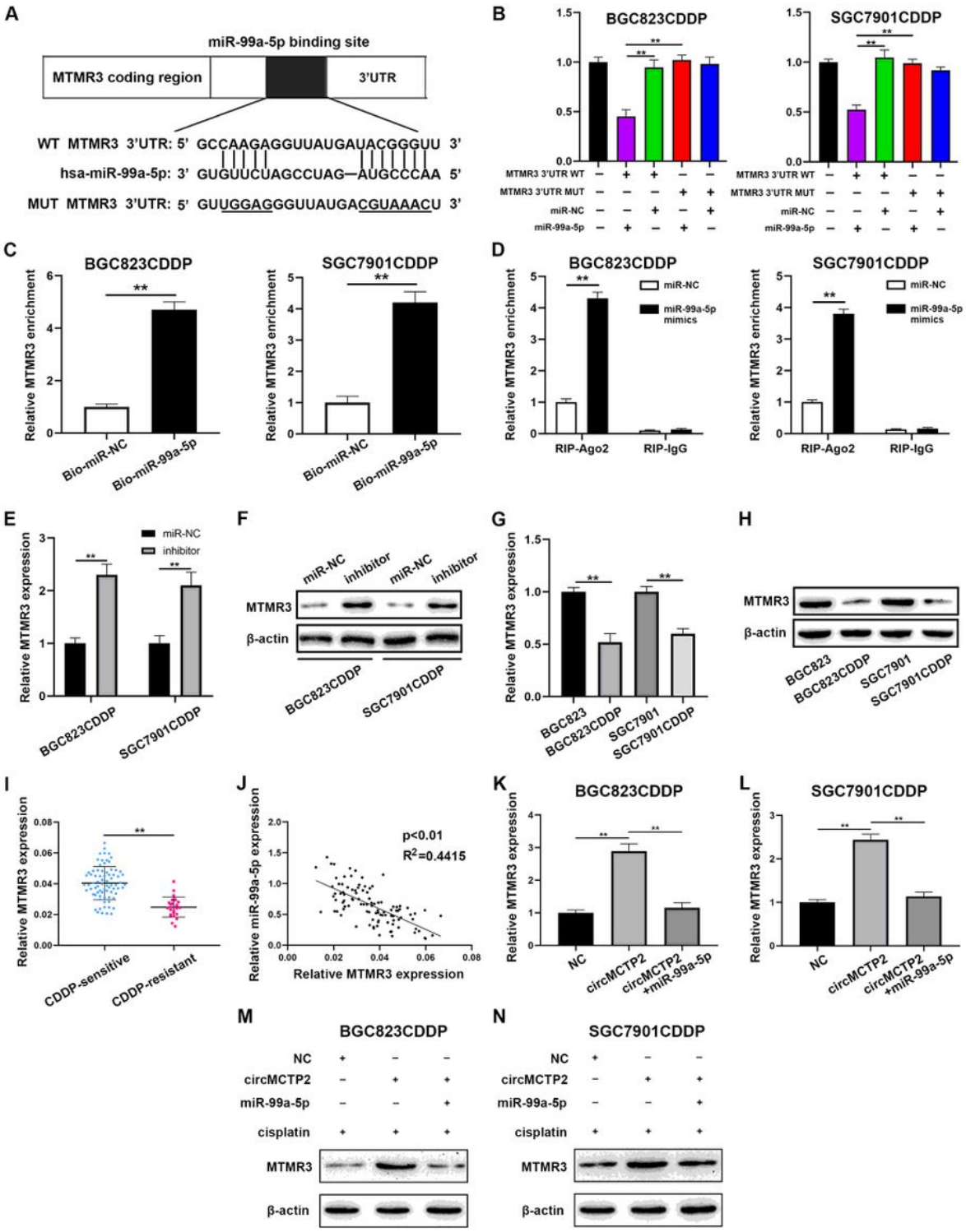

Figure 5

MTMR3 is a direct target of miR-99a-5p. a Potential binding site of miR-99a-5p for MTMR3 as predicted by Targetscan. b Luciferase reporter assay was performed to examine whether miR-99a-5p could bind to wt-MTMR3-3´UTR or mut-MTMR3-3´UTR. c Pull-down assay confirmed that MTMR3 was a target of miR-99a-5p. d RIP assay confirmed the interaction between miR-99a-5p and MTMR3. e Downregulation of miR-99a-5p could increase the expression levels of MTMR3, as detected by qRT-PCR. f Knockdown of miR-99a-5p increased the protein expression levels of MTMR3. g qRT-PCR was performed to detect the expression of MTMR3 CDDP-sensitive and CDDP-resistant GC cells. h MTMR3 was detected in CDDP-resistant and CDDP-sensitive GC cells by western blotting. i MTMR3 expression was detected using qRT-PCR in CDDP-sensitive and CDDP-resistant GC tissues. j MTMR3 expression was negatively corelated to the expression of miR-99a-5p. k and l MTMR3 expression was increased by circMCTP2 but was reversed by overexpression of miR-99a-5p, as confirmed by qRT-PCR. m and n The promotive effect of circMCTP2 on the protein expression of MTMR3 was diminished by the overexpression of miR-99a-5p. (*$p<0.05$, **$p<0.01$. Data expressed as mean ± SD).

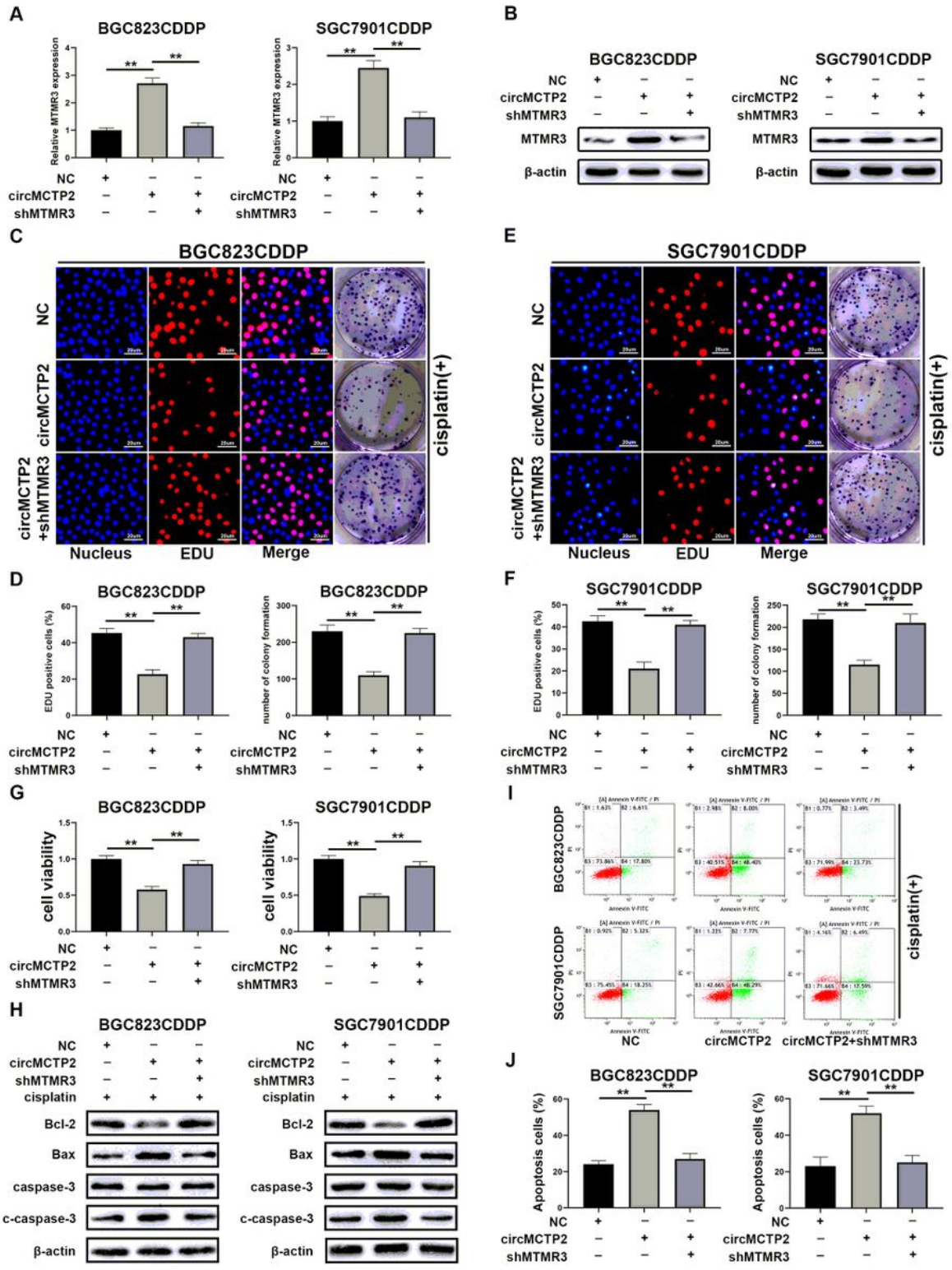

Figure 6

The effects of circMCTP2 can be reversed by the knockdown of MTMR3. a The expression levels of MTMR3 in BGC823CDDP and SGC7901CDDP after transfection with lentivirus-shMTMR3 were determined by qRT-PCR. b Protein expression levels of MTMR3 in BGC823CDDP and SGC7901CDDP were detected by western blotting. c and d Effects of circMCTP2 on cell proliferation and colony formation of BGC823CDDP were reversed by the knockdown of MTMR3. e and f Decreased cell proliferation and

colony forming ability of SGC7901CDDP caused by circMCTP2 were restored by the knockdown of MTMR3. g MTMR3 knockdown could reverse the effects of circMCTP2 on cell viability. h Expression levels of apoptotic proteins were examined by western blotting. i and j Flow cytometric analysis was performed to detect whether shMTMR3 could reverse the effect of circMCTP2 on apoptosis of BGC823CDDP and SGC7901CDDP. CDDP treatment: 12 μM, 48 h for BGC823CDDP and 6 μM, 48 h for SGC7901CDDP. (*p<0.05, **p<0.01. Data are expressed as mean ± SD).

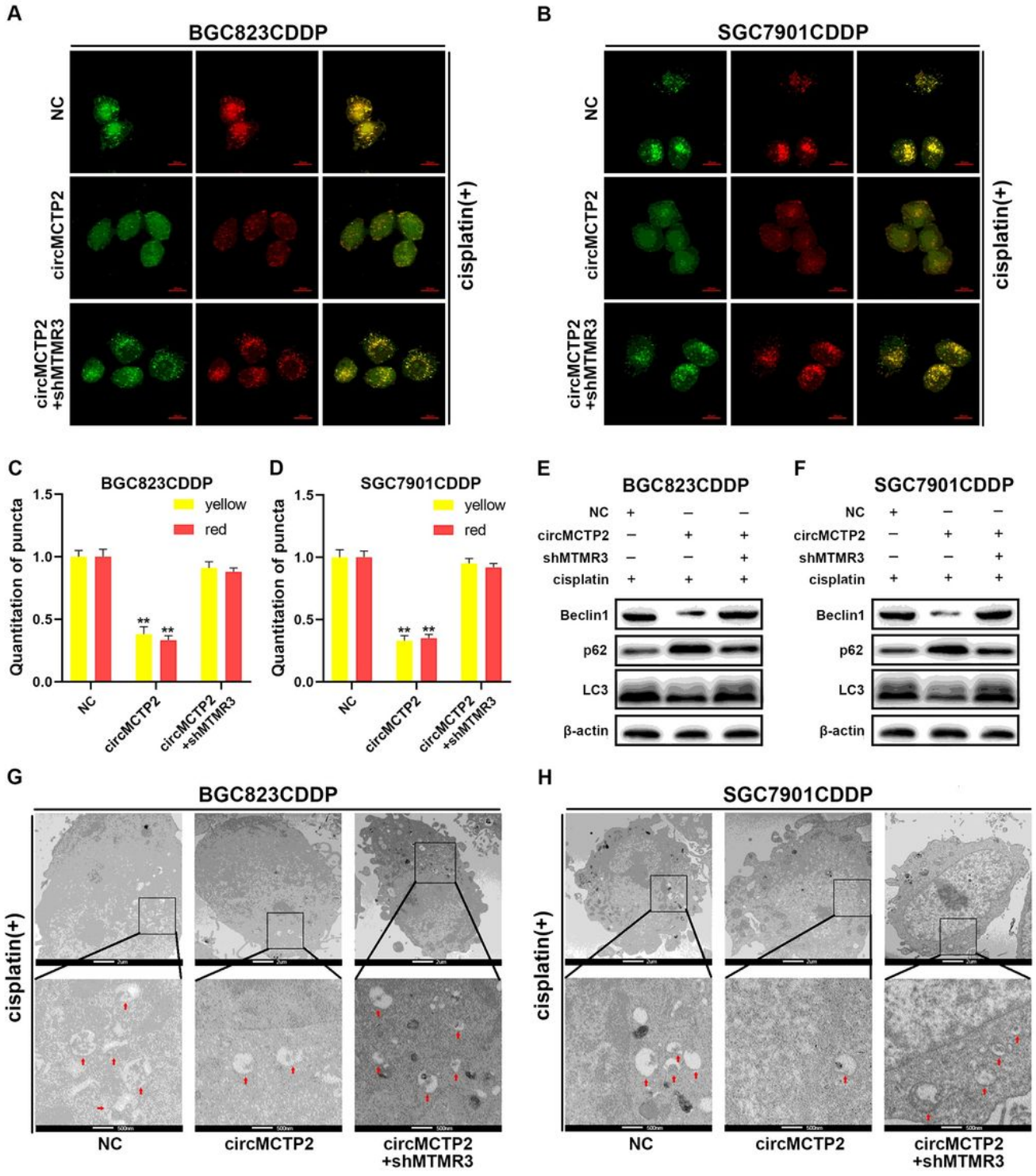

Figure 7

The effect of circMCTP2 on autophagy is reversed by the downregulation of MTMR3. a-d Confocal microscopy analysis showing the accumulation of GFP/mRFP-LC3 dots. e and f Western blotting showing the expression levels of Beclin1, p62, and LC3-II proteins. g and h TEM analysis showing the autophagic microstructure in CDDP-resistant GC cells. CDDP treatment: 12 μM, 48 h for BGC823CDDP and 6 μM, 48 h for SGC7901CDDP. (*p<0.05, **p<0.01. Data are expressed as mean ± SD).

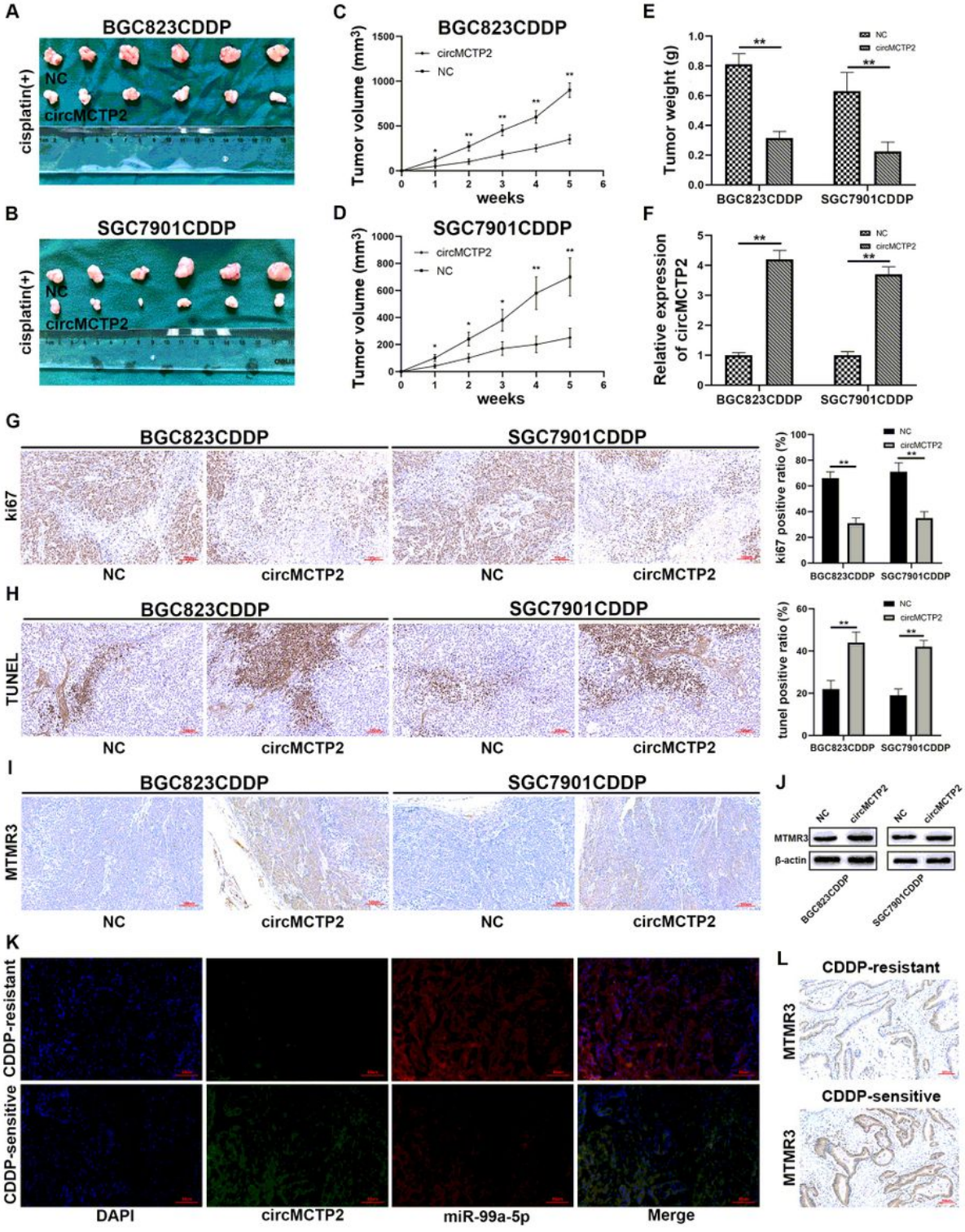

Figure 8

CircMCTP2 sensitizes GC cells to CDDP in vivo. a-d CircMCTP2 suppressed the growth of xenograft tumors with CDDP treatment. e Weight of xenograft tumors was measured. f CircMCTP2 expression was detected by qRT-PCR in xenograft tumors. g Percentage of ki67-positive cells in xenograft tumors was measured. h TUNEL assay was performed to determine the apoptosis of GC cells in nude mice tumors. i, j MTMR3 protein expression in xenograft tumors was examined by IHC and western blotting. k The expression levels of circMCTP2 and miR-99a-5p were detected by FISH assay in CDDP-resistant and CDDP-sensitive GC tissues. l The results of IHC revealed that MTMR3 was downregulated in CDDP-resistant GC tissues. (*p<0.05, **p<0.01. Data are expressed as mean ± SD).

Supplementary Files

This is a list of supplementary files associated with this preprint. Click to download.

- FigureS3.pdf
- FigureS2.pdf
- FigureS1.pdf
- TableS1.pdf